


Thermal transitions in serum amyloid A in solution and on the lipid: implications for structure and stability of acute-phase HDL [§]

Shobini Jayaraman,^{1,*} Christian Haupt,[†] and Olga Gursky^{1,*}

Department of Physiology & Biophysics,* Boston University School of Medicine, Boston MA 02118; and Institute for Pharmaceutical Biotechnology,[†] University of Ulm, 89081, Ulm, Germany

Abstract Serum amyloid A (SAA) is an acute-phase protein that circulates mainly on plasma HDL. SAA interactions with its functional ligands and its pathogenic deposition in reactive amyloidosis depend, in part, on the structural disorder of this protein and its propensity to oligomerize. In vivo, SAA can displace a substantial fraction of the major HDL protein, apoA-I, and thereby influence the structural remodeling and functions of acute-phase HDL in ways that are incompletely understood. We use murine SAA1.1 to report the first structural stability study of human plasma HDL that has been enriched with SAA. Calorimetric and spectroscopic analyses of these and other SAA-lipid systems reveal two surprising findings. First, progressive displacement of the exchangeable fraction of apoA-I by SAA has little effect on the structural stability of HDL and its fusion and release of core lipids. Consequently, the major determinant for HDL stability is the nonexchangeable apoA-I. A structural model explaining this observation is proposed, which is consistent with functional studies in acute-phase HDL. Second, we report an α -helix folding/unfolding transition in SAA in the presence of lipid at near-physiological temperatures.  This new transition may have potentially important implications for normal functions of SAA and its pathogenic misfolding.—Jayaraman, S., C. Haupt, and O. Gursky. Thermal transitions in serum amyloid A in solution and on the lipid: implications for structure and stability of acute-phase HDL. *J. Lipid Res.* 2015. 56: 1531–1542.

Supplementary key words high density lipoprotein • differential scanning calorimetry • circular dichroism spectroscopy • exchangeable apolipoprotein A-I • lipid-induced α -helix folding • thermodynamically irreversible transition • protein-lipid interactions

Serum amyloid A (SAA) is an acute-phase protein associated with plasma HDL. In acute infection, the plasma concentration of SAA can increase more than 1,000-fold reaching up to 1 mg/ml in 1–2 days and return to baseline levels in 7–10 days (1, 2). Thus, SAA acts as a positive acute-phase

reactant, and plasma levels of SAA provide a useful biomarker to assess the severity of the inflammation and the response to anti-inflammatory therapies (3). Persistently high levels of SAA can lead to amyloid A (AA) amyloidosis. This life-threatening complication of chronic inflammation in humans results from deposition of the N-terminal fragments of SAA, termed AA, in organs and tissues (4). The most abundant fragment found in deposits is 1–76 (5, 6). SAA isoforms are differentially expressed during inflammation. In the current work, we use SAA1.1, which is one of the major isoforms in humans and mice and a precursor of AA (7, 8).

Amino acid sequences of mammalian SAAs (12 kDa, 104 amino acids) are highly evolutionally conserved, suggesting conserved structures. In aqueous solution under near-physiological conditions these proteins are intrinsically disordered, yet they can acquire α -helical structure upon binding ligands such as lipids. High-resolution X-ray crystal structures of human SAA1.1 and murine SAA3 have recently been determined, providing the much-needed structural basis for elucidating functional properties of SAA such as binding to HDL and retinol, as well as self-association (9, 10). Although these proteins have been crystallized in different oligomeric forms (dimer, tetramer, or hexamer), they had a remarkably similar monomer fold, suggesting that this fold is conserved across the family. SAA monomer forms a funnel-shaped four-helix bundle, with the HDL binding site located at the apex of the N-terminal amphipathic α -helix and the flexible C-terminal tail wrapped around the bundle to stabilize it (9, 10).

Abbreviations: AA, amyloid A; CD, circular dichroism; CETP, cholesteryl ester transfer protein; DMPC, 1,2-dimyristoyl-*sn*-glycero-3-phosphocholine; DSC, differential scanning calorimetry; EM, electron microscopy; NDGE, nondenaturing gel electrophoresis; nHDL, normal HDL; PLA₂, phospholipase A₂; PLTP, phospholipid transfer protein; SAA, serum amyloid A; SAA-HDL, SAA-enriched HDL; SEC, size-exclusion chromatography; sPLA₂, secretory phospholipase A₂; SR-BI, scavenger receptor class B type I; SUV, small unilamellar vesicle.

[†]To whom correspondence should be addressed.

e-mail: shobini@bu.edu (S.J.); Gursky@bu.edu (O.G.)

[§]The online version of this article (available at <http://www.jlr.org>) contains supplementary data in the form of four figures.

This work was supported by National Institutes of Health Grant GM067260 (O.G. and S.J.); C.H. was supported by the German Research Foundation (DFG) Grant HA 7138/2-1.

Manuscript received 16 April 2015 and in revised form 13 May 2015.

Published, JLR Papers in Press, May 28, 2015

DOI 10.1194/jlr.M059162

Copyright © 2015 by the American Society for Biochemistry and Molecular Biology, Inc.

This article is available online at <http://www.jlr.org>

Although the functional role of SAA is subject of debate, various biological functions have been attributed to this protein. In addition to its putative role in immune response, SAA was proposed to modulate blood coagulation (11), monocyte and neutrophil chemotaxis (12), and HDL functions in cholesterol transport and metabolism (13–16). SAA is implicated in retinol transport (10), and elevated plasma SAA is a cardiovascular risk factor (17). Many aspects of normal functions of SAA and its pathological deposition in amyloid remain unclear and are intimately linked to HDL metabolism.

Plasma HDLs are heterogeneous nanoparticles (8–12 nm) composed of lipids and specific amphipathic proteins, termed apolipoproteins (apos). The proteins and polar lipids (mainly phospholipids and cholesterol) form the HDL surface, while apolar lipids (cholesteryl esters and triacylglycerols) are sequestered in the core. Plasma levels of HDL cholesterol and the major HDL protein, apoA-I, have long been known to correlate inversely with the risk of cardiovascular disease (18), although recent studies show that HDL quality is also very important (19, 20). The cardioprotective effect of HDL is attributed, in part, to its antioxidant, antithrombotic, and anti-inflammatory properties, but mainly to its central role in reverse cholesterol transport, which is the sole pathway for removal of excess cholesterol from peripheral cells such as arterial macrophages (21, 22). ApoA-I (28 kDa, 243 amino acids) plays a key functional role in this complex pathway and also forms an important structural scaffold on the HDL surface (23, 24). In normal HDL (nHDL), apoA-I constitutes ~70% of protein mass, apoA-II (77 amino acids) constitutes ~20%, and the remainder is composed of minor apolipoproteins (25). The biochemical composition of HDL can drastically change in inflammation upon upregulation of two major acute-phase proteins, SAA and secretory phospholipase A₂ (sPLA₂), which remodel HDL (26).

Studies in mice and humans show that, in the acute phase, SAA binds to HDL, displaces a large fraction of apoA-I and other minor proteins, and becomes the major HDL protein that can constitute up to 80% of the total protein content in HDL (27, 28). Although SAA-enriched HDLs (SAA-HDLs) have larger size, they are associated with denser HDL₃ fraction, which is consistent with higher protein content in acute-phase human HDL compared with nHDL (29). This situation differs from acute inflammation in SAA-deficient mice where the increase in HDL size results from increased lipid content (30, 31). Because apoA-I is the major functional protein on HDL that modulates several lipid-processing reactions, the displacement of a large fraction of apoA-I with SAA is expected to alter HDL lipid composition. In fact, acute-phase HDL is enriched in free cholesterol and depleted in cholesteryl esters, which is likely due to the depletion in apoA-I, the preferred cofactor for LCAT. Acute-phase HDL is also enriched in triglycerides and free fatty acids that are elevated in inflammation (31). Importantly, HDL plasma levels can decline up to 2-fold in acute inflammation (32). This decline may result either from potential destabilization of acute-phase HDLs, which would lead to their enhanced catabolism (33), or, more likely, from HDL processing by sPLA₂ (26).

Changes in the biochemical composition and plasma levels of acute-phase HDL, along with the displacement of

lipid-poor apoA-I, are expected to influence HDL functions, such as the efflux of cell cholesterol at the critical steps of reverse cholesterol transport. In fact, some studies report that HDL enrichment with SAA increased HDL binding to macrophages, decreased cholesterol efflux from macrophages, and increased uptake of cholesteryl ester (34, 35). Moreover, SAA-HDLs are ineffective mediators of cholesterol esterification by LCAT (36) and have reduced antioxidant potential (37). These reports suggest that SAA diminishes the antiatherogenic properties of HDL. However, the effects of SAA on HDL functions are not necessarily deleterious (26, 38). For instance, similar to apoA-I, lipid-free SAA promotes efflux of cholesterol and phospholipids from cells and, hence, is proposed to play a protective role in cholesterol removal from macrophages at the sites of inflammation (14, 26, 39). Interestingly, certain key functions of HDL in reverse cholesterol transport are relatively unaffected by the biochemical changes in acute-phase HDL; this includes the stimulation of cholesteryl ester transfer protein (CETP) or the net effect on cell cholesterol efflux (15). Thus, the complex effects of SAA on the protective properties of HDL are far from clear. Moreover, the effects of SAA on HDL structure, stability, and functional remodeling during reverse cholesterol transport remain unclear and are addressed in the current study.

Metabolism of normal HDL critically depends on HDL remodeling by plasma factors such as LCAT and other lipases, CETP and phospholipid transfer protein (PLTP), and HDL scavenger receptor class B type I (SR-BI). This remodeling alters the biochemical composition of HDL and increases its lipid load, thereby shifting the balance between the polar surface of HDL and its apolar core. This balance can be restored upon apolipoprotein dissociation and HDL fusion, which can be induced by LCAT, hepatic lipase, PLA₂, CETP, or PLTP (40–44). Similar to apoA-I dissociation in these reactions, SAA can also be released from acute-phase HDL upon the action of CETP, PLA₂, and other plasma factors (45). At the last step of reverse cholesterol transport, HDL disintegrates (or ruptures) and releases its core lipids that are taken up by the SR-BI receptor; this disintegration is accompanied by apolipoprotein dissociation (46). Notably, important aspects of metabolic HDL remodeling by plasma factors, including apoA-I dissociation and HDL fusion and rupture, are mimicked in chemical or thermal denaturation (47, 48). Therefore, we use thermal denaturation as a tractable experimental model to determine the effects of various HDL modifications on the functional remodeling of HDL (49).

Here, we combine several biochemical and biophysical methods to determine, for the first time, the effects of SAA enrichment on the HDL stability to heat-induced fusion and rupture. We report the first study of SAA in solution and on HDL using differential scanning calorimetry (DSC). To glean further insights into the molecular basis of the observed effects, we investigate the stability and conformational changes of SAA in the presence of lipids. A structural model of SAA-HDL is proposed that explains our findings. These findings may have important implications for understanding functional remodeling of acute-phase HDL as well as the normal functions of SAA and its pathological misfolding in amyloid.

MATERIALS AND METHODS

Proteins and lipids

Recombinant murine SAA1.1 (termed SAA for brevity) was expressed in *Escherichia coli* and purified as described elsewhere (50). Human apoA-I was isolated and purified to ~95% purity from plasma HDL and refolded as described (51). Monoclonal antibodies for apoA-I (#MAC20-001) and SAA (#H86177M) were purchased from Meridian Life Sciences. Both 1,2-dimyristoyl-*sn*-glycero-3-phosphocholine (DMPC; 14:0, 14:0) and POPC (16:0, 16:1) were purchased from Avanti Polar Lipids. All chemicals were of highest purity analytical grade.

Preparation and characterization of normal human plasma HDL and SAA-HDL

Plasma of healthy volunteer donors was purchased from Research Blood Components LLC, according to their rules and regulations and upon approval of the Institutional Review Board. Single-donor HDLs of healthy humans, termed nHDL, were isolated from fresh EDTA-treated plasma by KBr density gradient ultracentrifugation in the density range 1.08–1.21 g/l as previously described (48). HDL stock solution containing 10 mM Na phosphate buffer at pH 7.5 (which is a standard buffer used throughout this study) and 0.25 mM Na EDTA was stored in the dark at 4°C and was used within 4 weeks. To obtain SAA-HDL, nHDLs were incubated with SAA at 37°C for 3 h, during which the exchange reaction reached equilibrium (data not shown). No changes in the particle size, composition, or stability were detected in control HDL upon incubation. The SAA to apoA-I ratios ranged from 0:1 (control) to 4:1 mol/mol, or 1.7:1 mg/mg, which approximates the

range of relative protein concentrations found in plasma. In fact, in acute-phase plasma, SAA can reach up to 1 mg/ml, while apoA-I can decline 2-fold from its normal levels of 0.8–1.4 mg/ml (52, 53). Therefore, concentrations of 0.85 mg/ml SAA and 0.5 mg/ml apoA-I, which exemplify acute-phase plasma, correspond to 4:1 mol/mol SAA:apoA-I used in our studies.

To assess HDL remodeling upon incubation with SAA, total samples of nHDL and SAA-HDL were characterized by size-exclusion chromatography (SEC) controlled by an AKTA UPC 10 FPLC system (GE Healthcare), and by nondenaturing gel electrophoresis (NDGE) followed by immunoblotting for apoA-I. The results clearly show that a large fraction of apoA-I progressively dissociates from HDL upon incubation with SAA in a dose-dependent manner (Fig. 1). Thus, SEC data show that dissociated apoA-I is absent from nHDL, is present in SAA-HDL (2:1), and increases in SAA-HDL (4:1) where more than 50% of total apoA-I is dissociated (Fig. 1A). This result agrees with densitometry analysis of the immunoblot for apoA-I (Fig. 1C, D), which was carried out by using ImageJ software (54). The fraction of dissociated apoA-I increases from ~3% at 0.5:1 SAA:apoA-I molar ratio to more than 60% at 4:1 ratio (Fig. 1D). These and other data, such as SDS-PAGE quantification of SEC fractions of SAA-HDL (not shown), consistently show that at 4:1 SAA:apoA-I mol ratio, approximately two-thirds of all apoA-I is dissociated from HDL. To maintain the particle density in the HDL₃ range, a comparable or slightly larger amount of SAA must be associated with these particles. These results agree with previous in vitro studies in SAA-HDL obtained by incubation, as well as with protein analysis in acute-phase plasma HDL reporting that up to three-fourths of the total apoA-I can be displaced from these particles (52, 53).

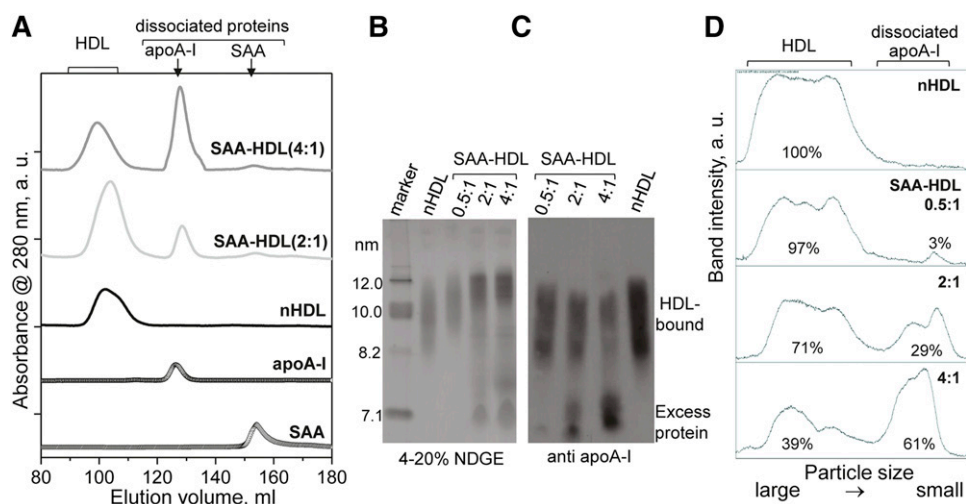


Fig. 1. Characterization of SAA-HDL by SEC and immunoblotting. A: SEC profiles of SAA-HDL using Superdex-200 preparative grade XK 16/100 column. Elution by PBS (10 mM Na phosphate, 150 mM NaCl, pH 7.5) was carried out at a flow rate of 1 ml/min. The data were recorded from nHDL and from SAA-HDL that have been incubated at 2:1 or 4:1 SAA:apoA-I molar ratio. The peaks corresponding to HDL-bound and dissociated proteins are indicated. Free apoA-I and SAA are shown for comparison. The data were shifted along the y-axis to avoid overlap. The relative peak intensities, which were obtained by integration using Unicorn software of AKTA, are proportional to weight % of total protein: 100% HDL-bound protein in nHDL; 83% HDL-bound protein and 17% dissociated apoA-I in SAA-HDL (2:1); 52% HDL-bound protein and 48% dissociated apoA-I in SAA-HDL (4:1). (B–D) Quantification of HDL-bound and dissociated apoA-I in SAA-HDL by immunoblotting. SAA-HDL (0.5:1 to 4:1 mol/mol of SAA:apoA-I as indicated) were analyzed by NDGE (B) followed by immunoblotting for apoA-I (C) and band quantification (D). NDGE shows progressive increase in HDL particle size with concomitant protein dissociation (C). Western blot shows progressive dissociation of apoA-I from HDL. The apoA-I content was quantified by ImageJ analysis of the Western blot (54). The area under the peak was calculated in the calibrated mode. The % fraction of protein in each band is indicated. The results suggest preferential displacement of apoA-I from small HDL.

Next, HDL and SAA-HDL that were intact or were subjected to controlled heating and cooling were characterized by SDS-PAGE, NDGE, and immunoblotting (described below), and by transmission electron microscopy (EM). For EM analysis, lipoproteins were negatively stained with Na phosphotungstate and were visualized under low-dose conditions in a CM12 transmission electron microscope (Philips Electron Optics) as previously described (47).

Protein complexes with DMPC and POPC vesicles

Model lipoproteins were reconstituted by incubating SAA or apoA-I with multilamellar vesicles of DMPC (1:4 w/w) overnight at 24°C following established protocols (51). The unbound lipids were pelleted by centrifugation. The lipid and protein content in the supernatant was quantified by Bartlett and BCA assays, respectively.

Homogenous small unilamellar vesicles (SUVs) of POPC, which were ~22 nm in size, were prepared by sonication following published protocols (55). SAA or apoA-I was mixed with SUVs at a protein:lipid molar ratio of 1:100 and was incubated at 37°C for 6–12 h. The protein-lipid complexes were analyzed by NDGE and negative-stain EM as previously described (51).

Gel electrophoresis and immunoblotting

For NDGE, Novex™ 4–20% Tris-glycine gels (Invitrogen) were loaded with 6 µg protein per lane and run to termination at 1,500 V-h under nonreducing conditions in Tris-glycine buffer. For SDS-PAGE, Novex™ 4–20% Tris-glycine gels were loaded with 5 µg protein per lane and run at 200 V for 1 h under denaturing conditions in SDS-Tris-glycine buffer. The gels were stained with Denville blue protein stain. For Western blotting, the proteins were separated either on native or on SDS gels and were transferred to a polyvinylidene difluoride membrane for 1 h at 100 V, 4°C. The membrane was blocked for 1 h in Tris-buffered saline/casein blocking buffer. The blots were probed with antibodies for apoA-I or SAA in blocking buffer for 1 h. The blots were washed three times for 10 min each and were visualized using the ECL system (NEN Life Science Products).

Thermal stability studies

Calorimetric data were recorded from protein or lipoprotein solutions using the VP-DSC microcalorimeter (MicroCal) as previously described (56). Sample concentrations ranged from 0.18 to 1.0 mg/ml protein in standard buffer. Briefly, the heat capacity data, $C_p(T)$, were recorded during sample heating from 5°C up to 120°C at a rate of 90°C/h. DSC data of SAA alone were normalized to protein concentration and are reported in units kcal/mol(SAA)×°C. DSC data of HDL, which contained a mixture of various proteins and lipids, are reported in units of cal/°C.

Circular dichroism (CD) data were obtained using an AVIV415 spectropolarimeter to monitor protein secondary structure, aromatic packing, and thermal stability. Far-UV CD spectra (185–250 nm) were recorded from protein or lipoprotein solutions in standard buffer. Far-UV CD data from samples containing only one protein (SAA or apoA-I) were normalized to protein concentration and expressed as molar residue ellipticity, $[\Theta]$. The CD data recorded from mixed protein systems, such as SAA-HDL, were not normalized and are reported in millidegrees. Protein α -helical content was assessed from the value of $[\Theta]$ at 222 nm, $[\Theta]_{222}$, using the formula % α -helix = $[-[\Theta]_{222} + 3,000]/39,000 \times 100$. Near-UV CD spectra (250–350 nm) are reported as molar ellipticity, Θ . Heat-induced changes were monitored at 222 nm for α -helical unfolding or at 280 nm for aromatic packing during sample heating and cooling at a rate of 70°C/h (fast) or 6°C/h (slow).

All experiments in this study were repeated three to five times to ensure reproducibility.

Temperature-dependent structural transitions in lipid-free SAA

First, we characterized the temperature dependence of the solution conformation of lipid-free SAA. Secondary structure and aromatic packing were monitored by far- and near-UV CD using 0.1 and 0.5 mg/ml protein, respectively. Far-UV CD spectra showed that SAA was ~33% α -helical at 5°C but largely unfolded at 25°C (Fig. 2A, insert) and fully unfolded at 37°C, as evident from the melting data (Fig. 2A) and the CD spectrum at 37°C (not shown). To monitor α -helical structure as a function of temperature, CD melting data were recorded at 222 nm. The results showed a sigmoidal unfolding transition centered at 18°C, which was largely reversible upon heating to 60°C and cooling to 5°C (Fig. 2A), in agreement with other SAA studies (57).

Near-UV CD spectra of free SAA at 5°C showed a negative peak at ~283 nm indicating Trp and/or Tyr packing resulting from tertiary and/or quaternary structure, which disappeared at 25°C (Fig. 2B, insert). Comparison of the melting data recorded at 222 nm and at 280 nm showed concomitant changes (Fig. 2A, B) indicating that the α -helical unfolding was accompanied by loss of aromatic packing. In addition to the protein unfolding below 30°C, irregular “bumps” in near-UV CD melting data were detected at 30°C–45°C, which were not accompanied by large far-UV CD changes (Fig. 2A, B) and probably reflected changes in protein oligomerization (described subsequently).

Structural transitions in lipid-free SAA were further explored by DSC. Fig. 2C shows consecutive heating scans from 10°C to 60°C recorded from the same sample containing 0.3 mg/ml SAA. An endothermic cooperative largely reversible transition centered at 36°C was observed between 30°C and 40°C. Because SAA is unfolded at these temperatures (Fig. 2A), this transition must reflect changes in protein self-association rather than secondary structure. DSC data recorded at various SAA concentrations support this conclusion. Although the calorimetric peak showed little change upon increasing SAA concentration from 0.18 to 0.3 mg/ml, further increase to 1.0 mg/ml SAA led to increased amplitude and a high-temperature shift of this peak (supplementary Fig. 1), supporting the idea that it involves changes in protein oligomerization. Further support comes from the previous studies reporting changes in SAA1.1 self-association at near-physiological temperatures (57, 58).

In sum, SAA heating to 30°C leads to nearly complete unfolding detected by far- and near-UV CD, followed by changes in protein self-association between 30°C and 40°C detected by DSC. These structural transitions are largely reversible.

Temperature-dependent structural transitions in SAA-HDL

To explore structural and stability properties of HDL that have been enriched with SAA, such as SAA-HDLs were prepared by using various SAA:apoA-I ratios as described in Materials and Methods and were analyzed for particle size, protein composition, conformation, and structural stability. As expected, NDGE and negative-stain EM showed

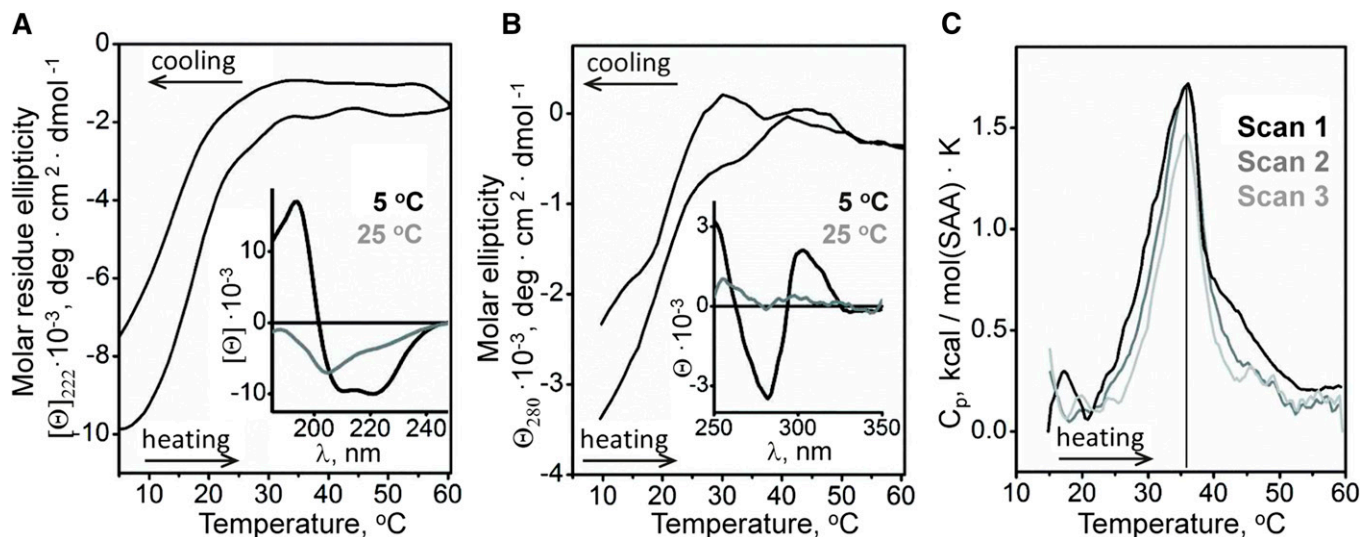


Fig. 2. Structural transitions in lipid-free SAA in solution analyzed by CD spectroscopy and DSC. A: Far-UV CD spectra of SAA at 5°C and 25°C (insert) and the melting data at 222 nm to monitor α -helical structure. B: Near-UV CD spectra of SAA at 5°C and 25°C (insert) and the melting data at 280 nm to monitor aromatic packing. C: Heat capacity $C_p(T)$ recorded in three consecutive DSC scans from the same sample containing 0.3 mg/ml SAA during heating from 10°C to 60°C at a rate of 90°C/h.

progressive increase in the particle size upon increasing SAA:apoA-I molar ratio from 0.5:1 to 2:1 to 4:1 (Fig. 3A, C). At 0.5:1 ratio, all protein comigrated with HDL on NDGE, while at 2:1 and 4:1 ratios, both HDL-bound and dissociated protein was detected (Fig. 3A, B).

Next, excess protein was removed by SEC from SAA-HDL that was prepared at 2:1 protein ratio as described in supplementary Fig. 2A, and the isolated lipoprotein-only fraction, termed SEC-HDL (2:1), was analyzed (Fig. 3A, right lane). Western blotting showed that SAA-HDL and SEC-HDL contained both SAA and apoA-I, and that the

dissociated protein also contained both SAA and apoA-I that was displaced from HDL (Figs. 1, 3B). SDS-PAGE confirmed these results and showed that SAA displaced a large fraction of apoA-I but not apoA-II from HDL (supplementary Fig. 2B). As a result, SAA and apoA-I became the major proteins in HDL-bound and in dissociated fractions. Protein quantification by SEC and immunoblotting shows that apoA-I is progressively displaced from HDL upon incubation with SAA in a dose-dependent manner (Fig. 1); at 4:1 mol/mol SAA:apoA-I, up to two-thirds of total apoA-I is displaced (Fig. 1D, bottom). These results agree with previous

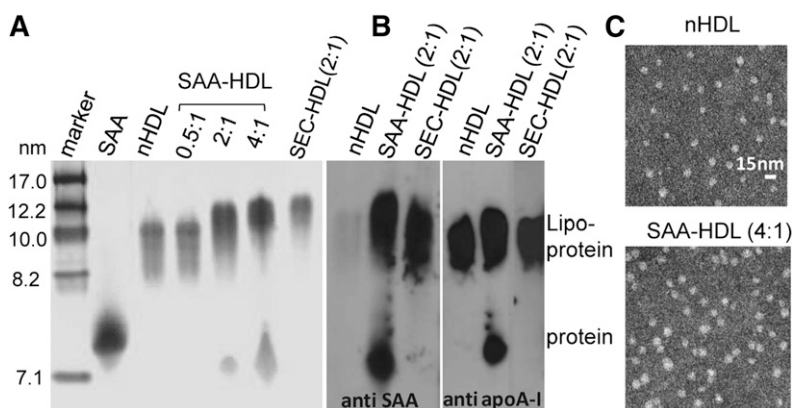


Fig. 3. Characterization of intact SAA-HDL by NDGE, immunoblotting, and negative-stain EM. A: NDGE of HDL incubated with SAA at molar ratios of SAA:apoA-I of 0.5:1 (nearly all protein is bound to HDL), 2:1 (part of apoA-I is displaced by SAA from HDL), and 4:1 (most apoA-I is displaced from HDL) (29, 63). SEC-HDL (2:1) stands for lipoprotein-only fraction isolated by SEC from SAA-HDL prepared using 2:1 ratio. All HDL samples contained 0.5 mg/ml apoA-I and varied amounts of SAA. Normal plasma HDL (nHDL) and lipid-free SAA are shown for comparison. The gels were stained with Denville blue protein stain. B: Western blots of SAA-HDL (2:1) and its lipoprotein-only fraction, SEC-HDL, show the distribution of the lipoprotein-bound and free SAA and apoA-I. nHDLs are shown for comparison. The gels were stained with Denville blue protein stain. C: Negative-stain electron micrographs of normal plasma HDL prior to incubation (top) or after incubation with SAA at 4:1 SAA:apoA-I molar ratio (bottom) are shown.

in vitro studies in SAA-HDL, as well as with protein analysis in acute-phase plasma HDL reporting that up to three-fourths of the total apoA-I can be displaced (52, 53). Thus, the protein composition in our in vitro studies in SAA-HDL is representative of the acute-phase plasma HDL.

Next, thermal stability and remodeling of SAA-HDL and nHDL were analyzed by DSC and NDGE (Fig. 4). Previously, we showed that HDL heating above 80°C leads to two irreversible kinetically controlled transitions: *i*) fusion into larger HDL-like particles accompanied by dissociation of a fraction of apoA-I; and *ii*) rupture of these particles, that is, lipoprotein disintegration, release of core lipids, and dissociation of lipid-poor apoA-I and apoA-II. Biochemical analysis of the products of this HDL transition was reported previously (48, 59). Consistent with these studies, DSC data in Fig. 4A show two high-temperature peaks in nHDL, which correspond to lipoprotein fusion and rupture. SAA-HDL showed similar DSC transitions (Fig. 4A) whose nature was confirmed by NDGE, immunoblotting, and EM. For example, SEC-HDLs have been heated to 50°C (well below the first high-temperature DSC peak), 95°C (above the first but below the second peak), or 110°C (above the second peak). NDGE showed that heating to 50°C did not cause HDL fusion, although some dissociation of SAA and apoA-I was detected by immunoblotting (not shown). Heating to 95°C led to increase in the particle size due to fusion accompanied by dissociation of a larger protein fraction (detected by NDGE; Fig. 4B) that comprised SAA and apoA-I (Western blot not shown). Further heating to 110°C led to lipoprotein disintegration and lipid coalescence into droplets, as indicated by NDGE (Fig. 4B) and EM (not shown). In sum, similar to nHDL, SAA-HDL also undergoes irreversible fusion, rupture, and apolipoprotein dissociation at high temperatures.

Compared with nHDL, SAA-HDL showed reduced amplitudes of these high-temperature DSC transitions, which reflected reduced amounts of apoA-I in these particles (Fig. 2) and perhaps less extensive apoA-I-lipid contacts, leading to reduced enthalpic contribution from apoA-I dissociation and unfolding. Surprisingly, the peak positions corresponding

to fusion and rupture of nHDL and of HDL that have been incubated with SAA were very similar, indicating similar structural stability of these particles (Fig. 4A).

Apart from the high-temperature transitions, DSC data of SAA-HDL showed an additional peak near 39°C (Fig. 4A). This peak did not involve irreversible changes in lipoprotein morphology or substantial protein dissociation, as indicated by NDGE of SAA-HDLs that have been heated to 50°C (Fig. 4B), although some protein dissociation was detected by immunoblotting. Notably, this peak was detected only in SAA-HDL, and its amplitude progressively increased upon increasing SAA concentration (Fig. 4A), suggesting that a structural transition in SAA was involved. An alternative explanation (i.e., that the peak reflected a transition in apoA-I that was progressively displaced from HDL) was dismissed because the lipid-free or lipid-poor apoA-I undergoes structural transitions at much higher temperatures approaching 60°C (59). Consequently, the 39°C peak reflected a structural transition in SAA that interacted with other HDL constituents. This SAA was probably bound to HDL, as suggested by the very similar peak observed in SEC-HDLs that contained only HDL-bound protein (SEC-HDL (2:1) in Fig. 4A; intact SEC-HDL (2:1) in Fig. 4B). The peak temperature and its shape did not change much upon increasing SAA concentration (Fig. 4A, vertical line), suggesting that this transition may involve either monomeric or oligomeric SAA.

In sum, we show for the first time that HDLs that have been incubated with SAA undergo fusion, rupture, and apolipoprotein dissociation that are similar to those in nHDLs and occur at similar temperatures. Consequently, despite the displacement of up to two-thirds of apoA-I with SAA, the structural stability and remodeling of the resulting SAA-HDL and nHDL are very similar. Another novel result is the calorimetric transition in SAA-HDL at near-physiological temperatures, which probably reflects structural transitions in SAA that interacts with HDL.

The structural basis for these transitions was further probed by CD spectroscopy (Fig. 5). Far-UV CD spectra in

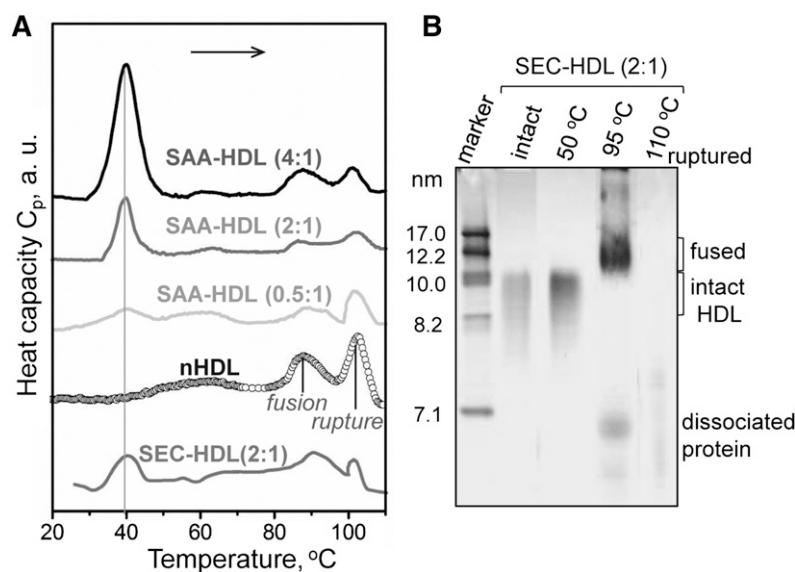


Fig. 4. Thermal denaturation of SAA-HDL analyzed by DSC and NDGE. A: DSC data of SAA-HDL were recorded during heating from 5°C to 120°C at a rate of 90°C/h. The samples contained 0.8 mg/ml apoA-I and various amounts of SAA at indicated SAA:apoA-I molar ratios. SEC-HDL is the lipoprotein-only fraction isolated by SEC from the total SAA-HDL (2:1 SAA:apoA-I). The data are shifted along the y-axis to avoid overlap. B: NDGE of SEC-HDLs that were intact or heated to 50, 95, or 110°C. Heating to 50°C does not cause HDL remodeling. Heating to 95°C causes partial protein dissociation and HDL fusion; Western blotting detects SAA and apoA-I both in fused HDL and in the dissociated protein (data not shown). Heating to 110°C causes lipoprotein disruption and coalescence into protein-containing lipid droplets that do not enter the gel. For more detailed biochemical analysis of the products of HDL thermal denaturation, see (59).

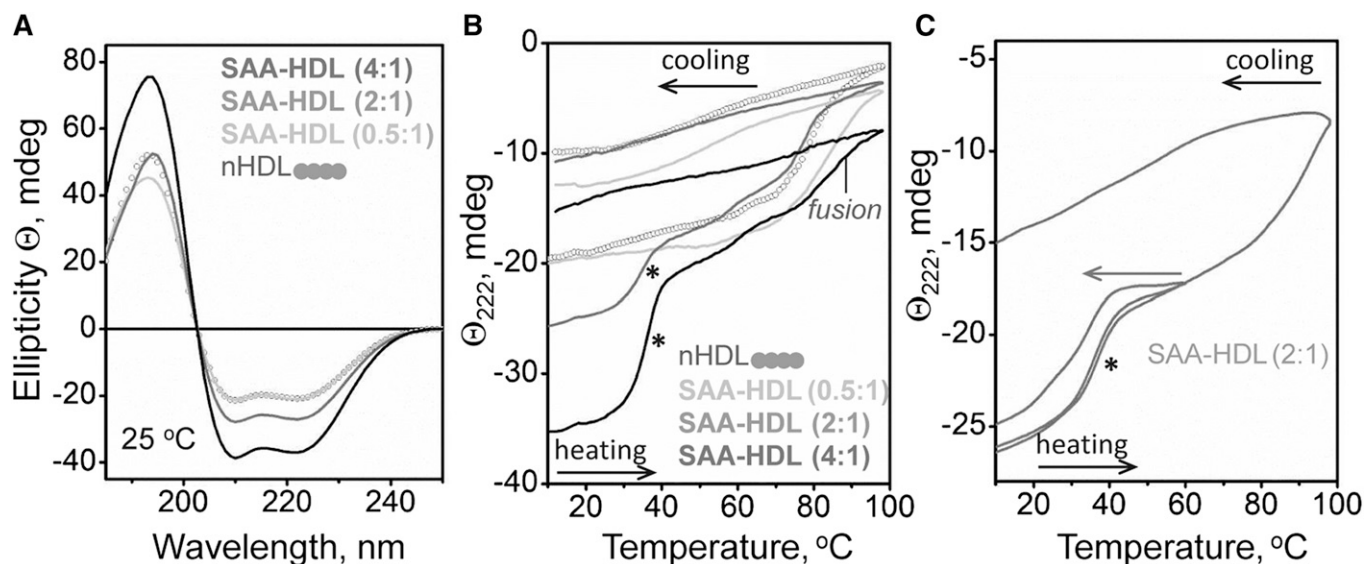


Fig. 5. Analysis of the heat-induced secondary structural changes in SAA-HDL by far-UV CD. HDLs (20 $\mu\text{g}/\text{ml}$ protein in standard buffer) have been incubated at indicated SAA:apoA-I molar ratios to generate SAA-HDL. The samples were placed in a 5 mm path length cell; the data were not normalized to protein concentration. **A:** Far-UV CD spectra of SAA-HDL at 25°C. **B:** Heating and cooling data, $\Theta_{222}(T)$, recorded at 222 nm at a scan rate of 6°C/h. Arrows show direction of temperature changes; asterisk indicates the unfolding transition at near-physiological temperatures. **C:** CD melting data recorded from two identical samples of SAA-HDL (2:1 SAA:apoA-I), one heated and cooled to 60°C and another to 98°C. The heating rate was 6°C/h.

Fig. 5A were recorded at 25°C from nHDL and from SAA-HDL by using a constant HDL concentration and increasing SAA to apoA-I ratios. The results showed formation of additional α -helical structure in SAA in the presence of HDL at 2:1 and 4:1 mol/mol SAA:apoA-I. Thus, in contrast to lipid-free SAA that is largely unfolded at 25°C (Fig. 2A), SAA acquires α -helical structure in the presence of HDL. Because α -helical content in human apoA-I is nearly 80% on HDL and 60% in solution, our CD data suggest that, at 4:1 molar (or 1.7:1 weight) ratio of SAA to apoA-I in SAA-HDL, the α -helical content in SAA reaches $\sim 35\%$. To probe the stability of this helical structure, heating and cooling data were recorded from SAA-HDL by CD at 222 nm (Fig. 5B). All samples showed irreversible thermal unfolding above 80°C, which corresponds to HDL fusion and dissociation and unfolding of an apoA-I fraction; this result is in good agreement with previous studies in nHDL (48). Furthermore, CD melting data indicate that nHDL and SAA-HDL undergo fusion at similar temperatures (Fig. 5B), in agreement with the DSC results (Fig. 4A).

Unexpectedly, SAA-HDL at 2:1 and 4:1 ratios showed an additional α -helical unfolding transition between 30°C and 40°C (Fig. 5B, marked by an asterisk). In contrast to irreversible HDL fusion and rupture at higher temperatures, this structural transition was largely reversible upon heating and cooling to 60°C (Fig. 5C). The latter is consistent with the absence of irreversible changes in HDL size at 50°C observed by NDGE (Fig. 4B) and EM (not shown). This novel α -helical transition at near-physiological temperatures increased in amplitude but not in temperature upon increasing the SAA:apoA-I ratio from 2:1 to 4:1. Interestingly, this transition was observed only in samples containing both HDL-bound and excess SAA. It was not detected in samples containing

only HDL-bound protein, such as SAA-HDL (0.5:1) (Fig. 5B) or HDL-only fraction isolated by SEC from SAA-HDL (2:1) (supplementary Fig. 3). This suggests that excess protein is involved in this transition and explains why it was missed in the previous studies that used isolated SAA-HDL.

To test the involvement of SAA in this novel transition, we used human apoA-II that, similar to SAA, can displace apoA-I from HDL [(60) and references therein]. HDLs have been incubated with apoA-II at 37°C for 3 h using 2:1 mol/mol apoA-II:apoA-I, and CD melting data were recorded (supplementary Fig. 4). Although significant amounts of apoA-I were displaced with apoA-II from these HDLs, the helical transition at near-physiological temperatures was lacking (supplementary Fig. 4), indicating that SAA is necessary for this transition to be observed.

Thermal denaturation of SAA:DMPC complexes

To further test the effect of lipid binding on SAA structure and stability, we reconstituted binary complexes of SAA with DMPC, termed SAA:DMPC. NDGE showed that all protein was incorporated into discrete complexes that were 9–19 nm in size, and negative-stain EM detected discoidal lipoproteins and small vesicles in this size range (Fig. 6A). Far-UV CD spectra of SAA:DMPC complexes indicated $\sim 50\%$ α -helix content at 5°C and at 25°C. Therefore, binding to DMPC stabilizes α -helical structure in SAA (Fig. 6B) as compared with free protein (Fig. 2A, insert). To test the stability of this structure, CD melting data were recorded at 222 nm from SAA:DMPC complexes during heating and cooling from 5°C to 98°C; similar data of apoA-I:DMPC complexes are shown for comparison (Fig. 6C). The heating curves showed cooperative α -helical unfolding in SAA:DMPC between 45°C and 55°C versus 80°C–90°C in

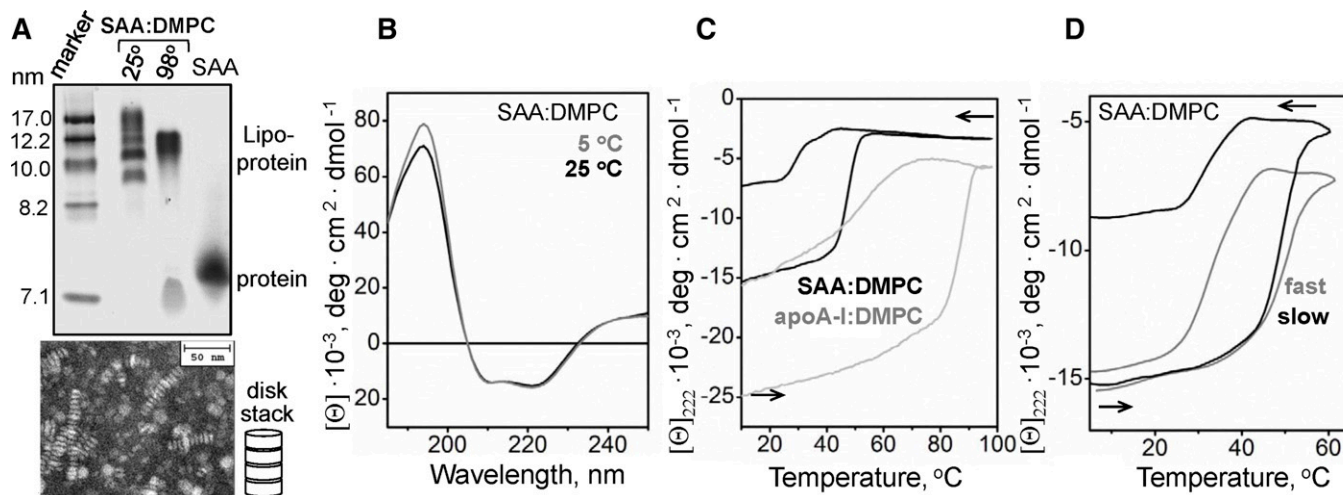


Fig. 6. Characterization of SAA:DMPC complexes. A: Reconstituted SAA:DMPC lipoproteins were analyzed by NDGE and negative-stain EM. Lane “25°” shows intact lipoproteins, and lane “98°” shows SAA:DMPC complexes that have been heated to 98°C and cooled to 25°C prior to analysis. B: Far-UV CD spectra of SAA:DMPC recorded at 5°C and 25°C. C: CD melting data of SAA:DMPC and apoA-I:DMPC complexes recorded at 222 nm during heating and cooling at a rate of 6°C/h. The apparent melting temperatures are indicated; asterisk indicates SAA refolding upon cooling at near-physiological temperatures. D: Scan rate effects on SAA:DMPC melting data. Heating and cooling CD data at 222 nm were recorded from two identical samples at a fast (70°C/h) and a slow (6°C/h) rate. The CD data are reported as molar residue ellipticity, $[\Theta]$.

apoA-I:DMPC, indicating much greater structural stability of the latter complexes. These results agree with a recent study showing that complex formation with DMPC increases the resistance of SAA to proteolysis and induces α -helical structure that unfolds upon heating near 50°C (61).

Notably, CD melting data of SAA:DMPC and apoA-I:DMPC showed hysteresis and incomplete signal recovery upon heating and cooling (Fig. 6C), indicating that the unfolding transition was thermodynamically irreversible. In contrast to the helical unfolding upon heating, which was centered at 49°C, helical refolding upon cooling occurred at near-physiological temperatures in SAA:DMPC (Fig. 6C). NDGE shows that heating and cooling of SAA:DMPC complexes beyond 90°C leads to their remodeling and dissociation of some SAA (Fig. 6A). Similar studies in other lipoproteins also showed a hysteresis and thermodynamic irreversibility, which was rooted in the partial unfolding and dissociation of lipid-poor apos accompanied by lipoprotein fusion (51, 59, 62). The results reported here suggest that similar effects occur in SAA:DMPC complexes.

Furthermore, the unfolding transition in SAA:DMPC complexes shifted to lower temperatures at slower heating rates: the apparent melting temperature, $T_{m,app}$, decreased from 49°C to 47°C upon slowing down the heating from 70°C to 6°C/h (Fig. 6D). This small but significant shift suggests low Arrhenius activation energy, E_a , of lipoprotein denaturation (62). Larger heating rate effects were observed in other similar complexes, indicating high activation energy of their denaturation ($E_a = 50$ kcal/mol for apoA-I:DMPC disks, with lower values observed for the complexes containing smaller proteins) (51). In sum, compared with apoA-I:DMPC, SAA:DMPC complexes show lower structural stability and lower apparent activation energy of denaturation, suggesting that SAA forms less extensive interactions with the lipid surface than apoA-I.

Thermal transition in SAA bound to POPC vesicles

Another model system used to test the effects of lipids on SAA conformation were SUVs of POPC. This zwitterionic phospholipid is an established model for the unsaturated phosphatidylcholines (PCs) found in HDL and in the plasma membrane. POPC SUVs were incubated with either SAA or apoA-I at 1:100 protein:lipid molar ratio at which the vesicle surface is expected to be saturated with the bound protein (54). NDGE of the incubation mixtures showed that most protein was bound to vesicles that were more than 20 nm in size (Fig. 7A, SAA-SUV). In addition, a small fraction of SAA remodeled SUVs into HDL-size particles (8–12 nm) that were similar in size to SAA:DMPC complexes. This fraction was not seen in apoA-I that does not spontaneously remodel POPC SUVs at a high enough rate; instead, excess apoA-I migrated as free protein (Fig. 7A, apoA-I-SUV). Far-UV CD spectra of SAA-SUVs suggested 38% α -helix at 5°C and at 25°C (Fig. 7B), and the CD melting data showed that this helical structure unfolded upon heating with $T_{m,app} \sim 50^\circ\text{C}$ and gradually refolded upon cooling to near-physiological temperatures (Fig. 7C). Similar experiments using apoA-I-SUV incubation mixture showed two unfolding transitions, one at 60°C and another at 85°C, which reflect the respective unfolding of free and SUV-bound apoA-I (Fig. 7C). This comparison illustrates once again that SAA:lipid complexes are less stable than their apoA-I-containing counterparts. Further, similar to other protein-lipid complexes, SAA-SUVs show hysteresis and scan rate dependence in their heating and cooling data, indicating a thermodynamically irreversible transition (Fig. 7D).

DISCUSSION

This is the first calorimetric analysis complemented by far- and near-UV CD analysis of SAA in lipid-free and HDL-bound

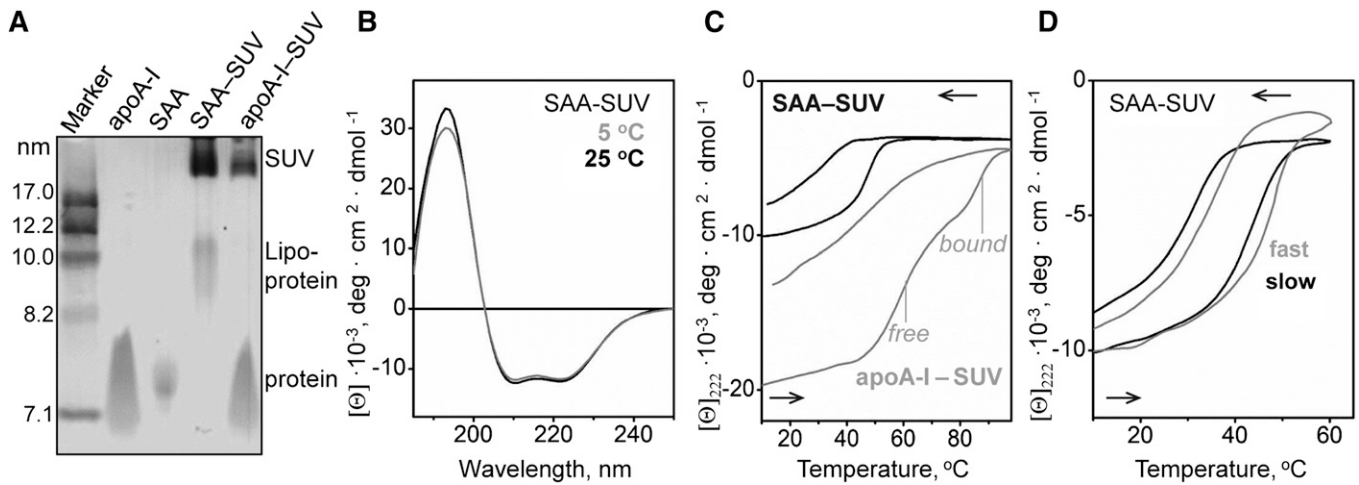


Fig. 7. Characterization of SAA complexes formed upon incubation with SUVs of POPC. SAA was incubated with POPC SUVs at 1:100 protein:lipid molar ratio to form SAA-SUVs. A: NDGE shows that all SAA was bound to lipid, either to SUV (~ 22 nm) or to SAA:POPC complexes in the HDL size range (9–11 nm). A similar sample containing apoA-I and POPC SUV, along with lipid-free apoA-I and SAA are shown for comparison. B: Far-UV CD spectra of SAA-SUV samples suggest similar helix content at 5°C and 25°C. C: CD heating and cooling data of POPC SUVs that have been incubated with SAA (black) or with apoA-I (gray) were recorded by CD at 222 nm. In intact samples, all SAA is lipid-bound, while apoA-I is distributed between lipid-bound and dissociated fractions whose thermal unfolding transitions are indicated. The data are in units of molar residue ellipticity, $[\Theta]$. D: Scan rate effects on the melting data of SAA-SUVs. The CD data at 222 nm were recorded from two identical samples at a fast (70°C/h) and a slow (6°C/h) rate.

forms and the first report on structural stability of SAA-containing human HDL. For free SAA1.1, we report a DSC transition near 39°C (Fig. 2C), which involves changes in the oligomerization degree of SAA that is devoid of ordered secondary structure at these temperatures (Fig. 2A). For SAA-HDL, we report two surprising findings. First, irreversible fusion and rupture of HDL, which occur above 80°C, are very similar in nHDL and in HDL that have been incubated with SAA in the wide range of SAA:apoA-I ratios explored, from 0:1 to 4:1 mol/mol (Fig. 3), which encompass the range found *in vivo* in normal and in acute-phase human plasma (28, 29, 31). Second, SAA-HDL shows a largely reversible cooperative helical folding/unfolding at near-physiological temperatures (Fig. 5B, C). This novel structural transition is observed in samples containing both excess protein and HDL and probably involves SAA that interacts with lipid. These two new findings are discussed in detail below.

Effects of apoA-I displacement on HDL stability

Surprisingly, the high-temperature transitions in human plasma HDL do not significantly change upon displacement of a large fraction of apoA-I (Figs. 4, 5). Even at 4:1 SAA:apoA-I molar ratio when roughly two-thirds of the total apoA-I is displaced (Fig. 1) (29, 63), the HDL transition temperatures remain nearly invariant (Fig. 4A). Therefore, the displacement of the exchangeable fraction of apoA-I has little effect on HDL stability to fusion and rupture. Consequently, the structural stability of human plasma HDL is determined primarily by the nonexchangeable fraction of apoA-I.

Previous studies proposed that structural remodeling of HDL induced by various perturbations (heating, denaturants, detergents, serum factors, etc.) mimics important aspects of HDL remodeling during reverse cholesterol transport (47, 48, 59). In fact, similar to biophysical perturbations,

HDL remodeling by plasma factors involves dissociation of lipid-poor apoA-I and HDL fusion (mediated by LCAT, hepatic lipase, PLA₂, PLTP, or CETP), followed by HDL rupture and release of core lipids (mediated by SR-BI receptor) and dissociation of the remaining apos (40–44). Therefore, our finding of similar structural stability in nHDL and in HDL that have been enriched with SAA is consistent with the finding that such enrichment *per se* does not reduce HDL levels in plasma (64). Together, these findings support the idea that decreased HDL levels in acute-phase response result from HDL hydrolysis by sPLA₂ rather than from HDL enrichment with SAA (26).

In contrast to plasma HDL, binary complexes of DMPC with apoA-I, which are established mimics of nascent HDL, are much more stable than those with SAA. Compared with apoA-I:DMPC, SAA:DMPC complexes undergo lipoprotein fusion and protein dissociation at much lower temperatures ($T_{m,app} \sim 85^\circ\text{C}$ for apoA-I:DMPC vs. 50°C for SAA:DMPC; Fig. 6C) and have lower apparent activation energy evident from the small scan rate effects on their melting data (Fig. 6D). These results suggest less extensive protein-lipid interactions in SAA:DMPC than in apoA-I:DMPC complexes, which can perhaps be explained by a relatively small SAA-lipid contact area involving the N-terminal α -helix that forms the primary HDL binding site in SAA (9) as compared with the much larger lipid binding surface formed by the apolar faces in the apoA-I α -helices that encircle HDL (21, 23, 65, 66).

Why do HDLs that have been incubated with SAA and nHDL have similar stability, whereas SAA:DMPC complexes are much less stable than their apoA-I-containing counterparts? The probable explanation is that, in contrast to SAA:DMPC complexes, SAA-HDLs contain not only SAA but also other proteins, mainly apoA-I and apoA-II. To explain why HDL stability does not significantly change upon

displacement of a large fraction of apoA-I with SAA, we propose a hypothetical structural model of SAA-HDL. This model is based on the double-belt conformation of apoA-I on HDL, which is widely accepted in the field and is supported by extensive experimental evidence, including the two available X-ray crystal structures of truncated forms of apoA-I (21, 23, 65, 66). We also rely on the modified trefoil/tetrafoil model first proposed by Davidson's group to explain how multiple copies of apoA-I can adapt their conformation to the surface of spherical HDL (67–69).

One possible model of intact HDL is illustrated in Fig. 8 (left). It shows four copies of apoA-I in a putative tetrafoil-like arrangement. SAA initially binds to the available HDL surface without displacing apoA-I (0.5:1 molar ratio). As SAA:apoA-I ratio increases, a progressive amount of apoA-I is displaced with SAA, until most exchangeable apoA-I is displaced at about 4:1 ratio (Fig. 8, left to right).

The presence of two populations of apoA-I on HDL, only one of which is readily exchangeable, was previously proposed to reflect the presence of two distinct apoA-I conformations [(60, 70, 71) and references therein]. Further, previous studies in model lipoproteins showed that smaller apos are generally more exchangeable than their larger counterparts; for example, under otherwise identical conditions human apoA-II monomer dissociates from the lipid much faster with only half the activation energy as compared with apoA-II dimer (51). Therefore, it is reasonable to assume that the exchangeable population of apoA-I on plasma HDL corresponds to protein monomer, while the nonexchangeable population corresponds to the double-belt

dimer (Fig. 8). Regardless of the exact structural model, the DSC and CD results reported here suggest that this nonexchangeable apoA-I is the key determinant of HDL stability to fusion and rupture (Figs. 4A, 5B).

Our stability studies are consistent with functional studies reporting that acute-phase HDLs have essentially intact functions in cell cholesterol efflux and CETP-mediated lipid transfer (15). Together, these studies suggest that the nonexchangeable fraction of apoA-I is the major determinant of the structural stability and functional remodeling of HDL in reverse cholesterol transport. We speculate that this important fraction is a double-belt apoA-I dimer.

SAA folding/unfolding at near-physiological temperatures

Another surprising finding of this study is the reversible α -helical folding/unfolding in SAA detected by CD at near-physiological temperatures in the presence of HDL (Fig. 5, asterisk). This helical transition is distinct from the calorimetric transition observed in lipid-free SAA at $\sim 36^\circ\text{C}$ (Fig. 2C), which involves changes in the oligomerization degree of SAA that is fully unfolded at near-physiological temperatures in the absence of the lipid (Fig. 2A). In contrast, SAA in the presence of HDL shows substantial α -helical structure ($\sim 34\%$) that unfolds with the midpoint at $\sim 38^\circ\text{C}$ (asterisk in Fig. 2B, C). Our results suggest that this helical transition involves SAA interacting with the lipid surface and occurs only in samples containing excess protein. In fact, this helical transition is not detected in lipid-free SAA (Fig. 2A) or in the lipid-containing samples that lack excess

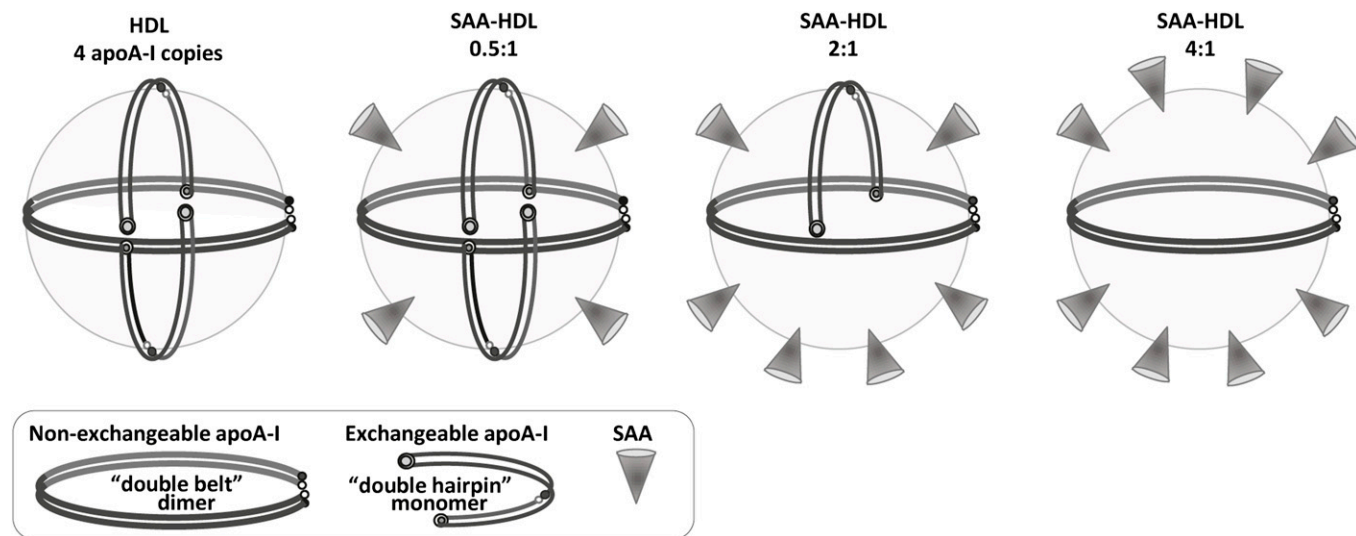



Fig. 8. Hypothetical structural model of mature plasma HDL containing increasing amounts of SAA. The model that exemplifies nHDL shows four copies of apoA-I, including one molecular dimer in a double-belt conformation and two monomers in a putative double-hairpin conformation. For details of these conformations and alternative models, see (69) and references therein. The SAA:apoA-I molar ratios are indicated. Addition of SAA initially leads to its binding to the available HDL surface (0.5:1 SAA:apoA-I mol/mol), followed by progressive displacement of the exchangeable fraction of apoA-I. We propose that this readily exchangeable apoA-I is probably monomeric, while the less exchangeable apoA-I that determines HDL stability is dimeric. HDL incubation at 4:1 molar (or 1.7:1 weight) ratio of SAA:apoA-I, which displaces approximately two-thirds of apoA-I from HDL (Fig. 1), must be compensated by binding of at least an equivalent amount of SAA in order to maintain the particle density in the HDL₃ range. Thus, the HDL-bound proteins comprise roughly two-thirds SAA and one-third apoA-I by weight, which resembles their ratio in the incubation mixture. Such a ratio of bound SAA to apoA-I can be achieved if HDL contains 2 apoA-I molecules and 8 to 10 SAA molecules (right panel).

protein, such as 0.5:1 SAA:apoA-I (when all protein is bound to HDL; Fig. 5B) or SEC-HDL from which the excess protein has been removed by SEC (supplementary Fig. 3). It is also not observed in the apoA-II-HDL sample despite the presence of excess apoA-I and HDL (supplementary Fig. 3), clearly indicating that SAA is involved.

These observations suggest that interactions of SAA with HDL and perhaps with the dissociated lipid-poor apoA-I can induce formation of a marginally stable helical structure in this intrinsically disordered protein. We hypothesize that reversible folding/unfolding of this helical structure at near-physiological temperatures (Fig. 5C) may modulate functional interactions of SAA with other proteins at the lipid surface and/or influence amyloid deposition. Studies in other proteins reported that, in contrast to the stable α -helical structure that inhibits amyloid formation, marginally stable α -helices (such as those formed in amyloid- β peptide and other intrinsically disordered proteins at the lipid surface) tend to promote intermolecular interactions leading to α -helix to β -sheet conversion in amyloid (72–74). The results of the current study prompt us to speculate that the precarious α -helical structure formed in SAA1.1 at the lipid surface may modulate local functional interactions of SAA at the sites of inflammation as well as its pathological deposition in amyloid. 

The authors thank Dr. Marcus Fändrich for many useful discussions and help providing murine SAA1.1, Dr. Nathan Meyers for preparing POPC vesicles, and Donald L. Gantz for help with EM.

REFERENCES

- Benditt, E. P., and N. Eriksen. 1977. Amyloid protein SAA is associated with high density lipoprotein from human serum. *Proc. Natl. Acad. Sci. USA* **74**: 4025–4028.
- Benditt, E. P., N. Eriksen, and R. H. Hanson. 1979. Amyloid protein SAA is an apoprotein of mouse plasma high density lipoprotein. *Proc. Natl. Acad. Sci. USA* **76**: 4092–4096.
- Kisilevsky, R., and P. N. Manley. 2012. Acute-phase serum amyloid A: perspectives on its physiological and pathological roles. *Amyloid* **19**: 5–14.
- Röcken, C., R. Menard, F. Bühling, S. Vöckler, J. Raynes, B. Stix, S. Krüger, A. Roessner, and T. Kähne. 2005. Proteolysis of serum amyloid A and AA amyloid proteins by cysteine proteases: cathepsin B generates AA amyloid proteins and cathepsin L may prevent their formation. *Ann. Rheum. Dis* **64**: 808–815.
- Röcken, C., and A. Shakespeare. 2002. Pathology, diagnosis and pathogenesis of AA amyloidosis. *Virchows Arch* **440**: 111–122.
- Westermarck, G. T., and P. Westermarck. 2010. Prion-like aggregates: infectious agents in human disease. *Trends Mol. Med* **16**: 501–507.
- Real de Asúa, D., R. Costa, J. M. Galván, M. T. Filigheddu, D. Trujillo, and J. Cadiñanos. 2014. Systemic AA amyloidosis: epidemiology, diagnosis, and management. *Clin. Epidemiol* **6**: 369–377.
- Srinivasan, S., S. Patke, Y. Wang, Z. Ye, J. Litt, S. K. Srivastava, M. M. Lopez, D. Kurouski, I. K. Lednev, R. S. Kane, et al. 2013. Pathogenic serum amyloid A 1.1 shows a long oligomer-rich fibrillation lag phase contrary to the highly amyloidogenic non-pathogenic SAA2.2. *J. Biol. Chem* **288**: 2744–2755.
- Lu, J., Y. Yu, I. Zhu, Y. Cheng, and P. D. Sun. 2014. Structural mechanism of serum amyloid A-mediated inflammatory amyloidosis. *Proc. Natl. Acad. Sci. USA* **111**: 5189–5194.
- Derebe, M. G., C. M. Zlatkov, S. Gattu, K. A. Ruhn, S. Vaishnav, G. E. Diehl, J. B. MacMillan, N. S. Williams, and L. V. Hooper. 2014. Serum amyloid A is a retinol binding protein that transports retinol during bacterial infection. *eLife* **3**: e03206.
- Zimlichman, S., A. Danon, I. Nathan, G. Mozes, and R. Shainkin-Kestenbaum. 1991. Serum amyloid A, an acute phase protein, inhibits platelet activation. *In* *Amyloid and Amyloidosis*. J. Natvig, Ø. Førre, G. Husby, A. Husebekk, B. Skogen, K. Sletten, and P. Westermarck, editors. Springer, Dordrecht, The Netherlands. 133–134.
- Badolato, R., J. M. Wang, W. J. Murphy, A. R. Lloyd, D. F. Michiel, L. L. Bausserman, D. J. Kelvin, and J. J. Oppenheim. 1994. Serum amyloid A is a chemoattractant: induction of migration, adhesion, and tissue infiltration of monocytes and polymorphonuclear leukocytes. *J. Exp. Med* **180**: 203–209.
- Annema, W., N. Nijstad, M. Tölle, J. F. de Boer, R. V. Buijs, P. Heeringa, M. van der Giet, and U. J. Tietge. 2010. Myeloperoxidase and serum amyloid A contribute to impaired in vivo reverse cholesterol transport during the acute phase response but not group IIA secretory phospholipase A(2). *J. Lipid Res* **51**: 743–754.
- Abe-Dohmae, S., K. H. Kato, Y. Kumon, W. Hu, H. Ishigami, N. Iwamoto, M. Okazaki, C-A. Wu, M. Tsujita, K. Ueda, et al. 2006. Serum amyloid A generates high density lipoprotein with cellular lipid in an ABCA1- or ABCA7-dependent manner. *J. Lipid Res* **47**: 1542–1550.
- Jahangiri, A., M. C. de Beer, V. Noffsinger, L. R. Tannock, C. Ramaiah, N. R. Webb, D. R. van der Westhuyzen, and F. C. de Beer. 2009. HDL remodeling during the acute phase response. *Arterioscler. Thromb. Vasc. Biol* **29**: 261–267.
- Stonik, J. A., A. T. Remaley, S. J. Demosky, E. B. Neufeld, A. Bocharov, and H. B. Brewer. 2004. Serum amyloid A promotes ABCA1-dependent and ABCA1-independent lipid efflux from cells. *Biochem. Biophys. Res. Commun* **321**: 936–941.
- Thompson, J. C., C. Jayne, J. Thompson, P. G. Wilson, M. H. Yoder, N. Webb, and L. R. Tannock. 2015. A brief elevation of serum amyloid A is sufficient to increase atherosclerosis. *J. Lipid Res* **56**: 286–293.
- Castelli, W. P. 1984. Epidemiology of coronary heart disease: the Framingham study. *Am. J. Med* **76**: 4–12.
- Rothblat, G. H., and M. C. Phillips. 2010. High-density lipoprotein heterogeneity and function in reverse cholesterol transport. *Curr. Opin. Lipidol* **21**: 229–238.
- Toth, P. P., P. J. Barter, R. S. Rosenson, W. E. Boden, M. J. Chapman, M. Cuchel, R. B. D'Agostino, Sr., M. H. Davidson, W. S. Davidson, J. W. Heinecke, et al. 2013. High-density lipoproteins: a consensus statement from the National Lipid Association. *J. Clin. Lipidol* **7**: 484–525.
- Phillips, M. C. 2014. Molecular mechanisms of cellular cholesterol efflux. *J. Biol. Chem* **289**: 24020–24029.
- Lund-Katz, S., and M. C. Phillips. 2010. High density lipoprotein structure-function and role in reverse cholesterol transport. *Subcell. Biochem* **51**: 183–227.
- Mei, X., and D. Atkinson. 2011. Crystal structure of C-terminal truncated apolipoprotein A-I reveals the assembly of high density lipoprotein (HDL) by dimerization. *J. Biol. Chem* **286**: 38570–38582.
- Phillips, M. C. 2013. New insights into the determination of HDL structure by apolipoproteins: thematic review series: high density lipoprotein structure, function, and metabolism. *J. Lipid Res* **54**: 2034–2048.
- Kontush, A., and M. J. Chapman. 2006. Functionally defective high-density lipoprotein: a new therapeutic target at the crossroads of dyslipidemia, inflammation, and atherosclerosis. *Pharmacol. Rev* **58**: 342–374.
- van der Westhuyzen, D. R., F. C. de Beer, and N. R. Webb. 2007. HDL cholesterol transport during inflammation. *Curr. Opin. Lipidol* **18**: 147–151.
- Malle, E., A. Steinmetz, and J. G. Raynes. 1993. Serum amyloid A (SAA): an acute phase protein and apolipoprotein. *Atherosclerosis* **102**: 131–146.
- Malle, E., and F. C. De Beer. 1996. Human serum amyloid A (SAA) protein: a prominent acute-phase reactant for clinical practice. *Eur. J. Clin. Invest* **26**: 427–435.
- Coetzee, G. A., A. F. Strachan, D. R. Vanderwesthuyzen, H. C. Hoppe, M. S. Jeenah, and F. C. Debeer. 1986. Serum amyloid A-containing human high density lipoprotein 3. Density, size, and apolipoprotein composition. *J. Biol. Chem* **261**: 9644–9651.
- de Beer, M. C., N. R. Webb, J. M. Wroblewski, V. P. Noffsinger, D. L. Rateri, A. Ji, D. R. van der Westhuyzen, and F. C. de Beer. 2010. Impact of serum amyloid A on high density lipoprotein composition and levels. *J. Lipid Res* **51**: 3117–3125.
- Cabana, V. G., J. R. Lukens, K. S. Rice, T. J. Hawkins, and G. S. Getz. 1996. HDL content and composition in acute phase response

- in three species: triglyceride enrichment of HDL a factor in its decrease. *J. Lipid Res.* **37**: 2662–2674.
32. Tietge, U. J. F., C. Maugeais, S. Lund-Katz, D. Grass, F. C. deBeer, and D. J. Rader. 2002. Human secretory phospholipase A(2) mediates decreased plasma levels of HDL cholesterol and ApoA-I in response to inflammation in human ApoA-I transgenic mice. *Arterioscler. Thromb. Vasc. Biol.* **22**: 1213–1218.
 33. Rye, K. A., and M. N. Duong. 2000. Influence of phospholipid depletion on the size, structure, and remodeling of reconstituted high density lipoproteins. *J. Lipid Res.* **41**: 1640–1650.
 34. Artl, A., G. Marsche, S. Lestavel, W. Sattler, and E. Malle. 2000. Role of serum amyloid A during metabolism of acute-phase HDL by macrophages. *Arterioscler. Thromb. Vasc. Biol.* **20**: 763–772.
 35. Cai, L., M. C. de Beer, F. C. de Beer, and D. R. van der Westhuyzen. 2005. Serum amyloid A is a ligand for scavenger receptor class B type I and inhibits high density lipoprotein binding and selective lipid uptake. *J. Biol. Chem.* **280**: 2954–2961.
 36. Steinmetz, A., G. Hocke, R. Saïle, P. Puchois, and J.-C. Fruchart. 1989. Influence of serum amyloid A on cholesterol esterification in human plasma. *Biochim. Biophys. Acta.* **1006**: 173–178.
 37. Van Lenten, B. J., S. Y. Hama, F. C. de Beer, D. M. Stafforini, T. M. McIntyre, S. M. Prescott, B. N. La Du, A. M. Fogelman, and M. Navab. 1995. Anti-inflammatory HDL becomes pro-inflammatory during the acute phase response. Loss of protective effect of HDL against LDL oxidation in aortic wall cell cocultures. *J. Clin. Invest.* **96**: 2758–2767.
 38. Navab, M., G. M. Anantharamaiah, S. T. Reddy, B. J. Van Lenten, B. J. Ansell, and A. M. Fogelman. 2006. Mechanisms of disease: proatherogenic HDL—an evolving field. *Nat. Clin. Pract. Endocrinol. Metab.* **2**: 504–511.
 39. van der Westhuyzen, D. R., L. Cai, M. C. de Beer, and F. C. de Beer. 2005. Serum amyloid A promotes cholesterol efflux mediated by scavenger receptor B-I. *J. Biol. Chem.* **280**: 35890–35895.
 40. Rye, K. A., M. A. Clay, and P. J. Barter. 1999. Remodelling of high density lipoproteins by plasma factors. *Atherosclerosis.* **145**: 227–238.
 41. Silver, E. T., D. G. Scرابا, and R. O. Ryan. 1990. Lipid transfer particle-induced transformation of human high density lipoprotein into apolipoprotein A-I-deficient low density particles. *J. Biol. Chem.* **265**: 22487–22492.
 42. Lusa, S., M. Jauhainen, J. Metso, P. Somerharju, and C. Ehnholm. 1996. The mechanism of human plasma phospholipid transfer protein-induced enlargement of high-density lipoprotein particles: evidence for particle fusion. *Biochem. J.* **313** (Pt. 1): 275–282.
 43. Liang, H. Q., K. A. Rye, and P. J. Barter. 1996. Remodelling of reconstituted high density lipoproteins by lecithin: cholesterol acyltransferase. *J. Lipid Res.* **37**: 1962–1970.
 44. Rye, K. A., N. J. Hime, and P. J. Barter. 1997. Evidence that cholesteryl ester transfer protein-mediated reductions in reconstituted high density lipoprotein size involve particle fusion. *J. Biol. Chem.* **272**: 3953–3960.
 45. Jahangiri, A. 2010. High-density lipoprotein and the acute phase response. *Curr. Opin. Endocrinol. Diabetes Obes.* **17**: 156–160.
 46. Silver, D. L., N. Wang, X. Xiao, and A. R. Tall. 2001. High density lipoprotein (HDL) particle uptake mediated by scavenger receptor class B type 1 results in selective sorting of HDL cholesterol from protein and polarized cholesterol secretion. *J. Biol. Chem.* **276**: 25287–25293.
 47. Mehta, R., D. L. Gantz, and O. Gursky. 2003. Human plasma high-density lipoproteins are stabilized by kinetic factors. *J. Mol. Biol.* **328**: 183–192.
 48. Jayaraman, S., D. L. Gantz, and O. Gursky. 2006. Effects of salt on the thermal stability of human plasma high-density lipoprotein. *Biochemistry.* **45**: 4620–4628.
 49. Guha, M., X. Gao, S. Jayaraman, and O. Gursky. 2008. Correlation of structural stability with functional remodeling of high-density lipoproteins: the importance of being disordered. *Biochemistry.* **47**: 11393–11397.
 50. Gellermann, G. P., T. R. Appel, A. Tannert, A. Radestock, P. Hortschansky, V. Schroeckh, C. Leisner, T. Lutkepohl, S. Shtrasburg, C. Rocken, et al. 2005. Raft lipids as common components of human extracellular amyloid fibrils. *Proc. Natl. Acad. Sci. USA.* **102**: 6297–6302.
 51. Jayaraman, S., D. L. Gantz, and O. Gursky. 2005. Kinetic stabilization and fusion of apolipoprotein A-2:DMPC disks: comparison with apoA-I and apoC-I. *Biophys. J.* **88**: 2907–2918.
 52. Gabay, C., and I. Kushner. 1999. Acute-phase proteins and other systemic responses to inflammation. *N. Engl. J. Med.* **340**: 448–454.
 53. Coetzee, G. A., A. F. Strachan, D. R. van der Westhuyzen, H. C. Hoppe, M. S. Jeenah, and F. C. de Beer. 1986. Serum amyloid A-containing human high density lipoprotein. *J. Biol. Chem.* **261**: 9644–9651.
 54. Abràmoff, M. D., P. J. Magalhães, and S. J. Ram. 2004. Image processing with ImageJ. *Biophotonics Int.* **11**: 36–42.
 55. McLean, L. R., and M. C. Phillips. 1984. Cholesterol transfer from small and large unilamellar vesicles. *Biochim. Biophys. Acta.* **776**: 21–26.
 56. Jayaraman, S., R. Jasuja, M. N. Zakharov, and O. Gursky. 2011. Pressure perturbation calorimetry of lipoproteins reveals an endothermic transition without detectable volume changes. Implications for adsorption of apolipoprotein to a phospholipid surface. *Biochemistry.* **50**: 3919–3927.
 57. Patke, S., S. Srinivasan, R. Maheshwari, S. K. Srivastava, J. J. Aguilera, W. Colon, and R. S. Kane. 2013. Characterization of the oligomerization and aggregation of human serum amyloid A. *PLoS ONE.* **8**: e64974.
 58. Linke, R. P. 1979. Temperature-induced dissociation of serum amyloid protein SAA. *Z. Immunitätsforsch. Immunobiol.* **155**: 255–261.
 59. Jayaraman, S., G. Cavigliolo, and O. Gursky. 2012. Folded functional lipid-poor apolipoprotein A-I obtained by heating of high-density lipoproteins: relevance to high-density lipoprotein biogenesis. *Biochem. J.* **442**: 703–712.
 60. Gao, X., S. Yuan, S. Jayaraman, and O. Gursky. 2012. Role of apolipoprotein A-II in the structure and remodeling of human high-density lipoprotein (HDL): protein conformational ensemble on HDL. *Biochemistry.* **51**: 4633–4641.
 61. Takase, H., H. Furuchi, M. Tanaka, T. Yamada, K. Matoba, K. Iwasaki, T. Kawakami, and T. Mukai. 2014. Characterization of reconstituted high-density lipoprotein particles formed by lipid interactions with human serum amyloid A. *Biochim. Biophys. Acta.* **1842**: 1467–1474.
 62. Gursky, O., Ranjana, and D. L. Gantz. 2002. Complex of human apolipoprotein C-I with phospholipid: thermodynamic or kinetic stability? *Biochemistry.* **41**: 7373–7384.
 63. Cabana, V. G., J. N. Siegel, and S. M. Sabesin. 1989. Effects of the acute phase response on the concentration and density distribution of plasma lipids and apolipoproteins. *J. Lipid Res.* **30**: 39–49.
 64. Hosoai, H., N. R. Webb, J. M. Glick, U. J. Tietge, M. S. Purdom, F. C. de Beer, and D. J. Rader. 1999. Expression of serum amyloid A protein in the absence of the acute phase response does not reduce HDL cholesterol or apoA-I levels in human apoA-I transgenic mice. *J. Lipid Res.* **40**: 648–653.
 65. Borhani, V. G., D. P. Rogers, J. A. Engler, and C. G. Brouillette. 1997. Crystal structure of truncated human apolipoprotein A-I suggests a lipid-bound conformation. *Proc. Natl. Acad. Sci. USA.* **94**: 12291–12296.
 66. Brouillette, C. G., G. M. Anantharamaiah, J. A. Engler, and D. W. Borhani. 2001. Structural models of human apolipoprotein A-I: a critical analysis and review. *Biochim. Biophys. Acta.* **1531**: 4–46.
 67. Silva, R. A., R. Huang, J. Morris, J. Fang, E. O. Gracheva, G. Ren, A. Kontush, W. G. Jerome, K. A. Rye, and W. S. Davidson. 2008. Structure of apolipoprotein A-I in spherical high density lipoproteins of different sizes. *Proc. Natl. Acad. Sci. USA.* **105**: 12176–12181.
 68. Huang, R., R. A. Silva, W. G. Jerome, A. Kontush, M. J. Chapman, L. K. Curtiss, T. J. Hodges, and W. S. Davidson. 2011. Apolipoprotein A-I structural organization in high-density lipoproteins isolated from human plasma. *Nat. Struct. Mol. Biol.* **18**: 416–422.
 69. Gursky, O. 2013. Crystal structure of $\Delta(185-243)$ ApoA-I suggests a mechanistic framework for the protein adaptation to the changing lipid load in good cholesterol: from flatland to sphereland via double belt, belt buckle, double hairpin and trefoil/tetrafoil. *J. Mol. Biol.* **425**: 1–16.
 70. Pownall, H. J. 2005. Remodeling of human plasma lipoproteins by detergent perturbation. *Biochemistry.* **44**: 9714–9722.
 71. Han, M., B. K. Gillard, H. S. Courtney, K. Ward, C. Rosales, H. Khant, S. J. Ludtke, and H. J. Pownall. 2009. Disruption of human plasma high-density lipoproteins by streptococcal serum opacity factor requires labile apolipoprotein A-I. *Biochemistry.* **48**: 1481–1487.
 72. Bennett, M. J., M. R. Sawaya, and D. Eisenberg. 2006. Deposition diseases and 3D domain swapping. *Structure.* **14**: 811–824.
 73. Fezoui, Y., and D. B. Teplow. 2002. Kinetic studies of amyloid beta-protein fibril assembly. Differential effects of alpha-helix stabilization. *J. Biol. Chem.* **277**: 36948–36954.
 74. Uversky, V. N. 2015. Protein misfolding in lipid-mimetic environments. *Adv. Exp. Med. Biol.* **855**: In press.